

# Kinetic and Mechanistic Parameters of Laccase Catalyzed Direct Electrochemical Oxygen Reduction Reaction

Naga S. Parimi,<sup>†</sup> Yogeswaran Umasankar,<sup>†</sup> Plamen Atanasov,<sup>‡</sup> and Ramaraja P. Ramasamy<sup>\*,†</sup>

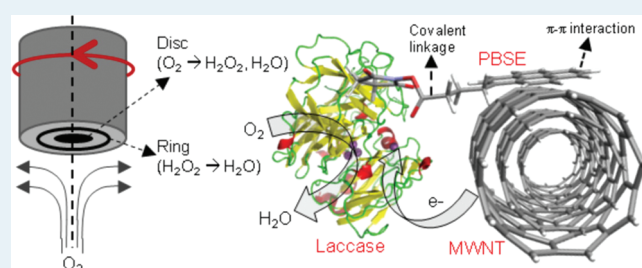
<sup>†</sup>Nano Electrochemistry Laboratory, Nanoscale Science and Engineering Center and Faculty of Engineering, University of Georgia, Athens, Georgia 30602, United States

<sup>‡</sup>Center for Emerging Energy Technologies, Department of Chemical and Nuclear Engineering, University of New Mexico, Albuquerque, New Mexico 87131, United States

## Supporting Information

**ABSTRACT:** This article presents the kinetic studies of oxygen reduction by one of the most important multicopper oxidases (fungal laccase) using the classic tool of electrochemistry: rotating ring-disk electrode (RRDE). Laccase was immobilized on a multiwalled carbon nanotube (MWNT) modified inert disk electrode using 1-pyrenebutanoic acid succinimidyl ester (PBSE), as a tethering agent. The conditions for laccase immobilization on MWNT were optimized to prepare a highly active composite electro-catalyst for O<sub>2</sub> reduction. The mechanistic as well as kinetic parameters such as Tafel slopes, number of electrons transferred, electrochemical rate constants (for heterogeneous charge transfer) and electron transfer rate constant were calculated from the RRDE experiment results. The Tafel slope obtained was close to the value of that of ideal four-electron reduction of O<sub>2</sub> to water indicating a highly active laccase in the tethered composite. The RRDE results also suggested the presence of intermediate steps in the oxygen reduction reaction. A model pathway for O<sub>2</sub> reduction reaction at the laccase composite modified electrode was postulated, and rate constants for individual reactions in the pathway were calculated. The rate constant for four-electron O<sub>2</sub> reduction was determined to be  $1.46 \times 10^{-3} \text{ mol s}^{-1}$ , indicating excellent electro-catalytic activity of the laccase-MWNT composite catalyst.

**KEYWORDS:** electrochemical kinetics, laccase, oxygen reduction, bioelectro-catalysis, biological fuel cell



## INTRODUCTION

The electrochemical reduction of oxygen to water is one of the most important reactions in electro-catalysis. Understanding the mechanism of this reaction has huge implications in the field of fuel cells and sensors. Fundamental electro-kinetic studies are essential to understand the mechanism and characteristics of this reaction. Such studies have been reported for oxygen reduction using various metal catalysts. For example one can point to the classic work by Damjanovic et al.,<sup>1–4</sup> who studied the oxygen reduction reaction (ORR) extensively on platinum surfaces. Similarly Savinell et al. and Srinivasan et al. have studied this reaction on various fuel cell electrodes and reported some electrochemical parameters.<sup>5–8</sup> These publications along with other relevant literature published later,<sup>9–11</sup> provide a quantitative method of analysis to evaluate the electrochemical activity of various metal catalysts for ORR, particularly for fuel cell application. Recently, a comprehensive and analytical summary of the kinetics of ORR by enzyme catalysts in comparison to the platinum and nonplatinum group metal catalysts has been presented by Gewirth and Thorum.<sup>12</sup> The use of enzymes as O<sub>2</sub> reduction catalysts has huge implications for biological fuel cells and biosensors.<sup>13</sup> The critical issues in enzyme electro-catalysis are the low active site loading (geometric area basis) and

insufficient electrical communication between enzyme redox center and electrode. The former is due to the large size of the enzyme compared to metallic catalyst centers, and the latter is due to the electrical insulation of the enzyme redox center by the surrounding protein matrix.<sup>14</sup> A common strategy to overcome the former issue is to composite the enzyme with nanomaterials to increase the surface area and hence the catalytic loading.<sup>15–19</sup> Among various nanomaterials used for this purpose, multiwalled carbon nanotubes (MWNTs) possess high electrical conductivity and large surface area for enzyme immobilization. In evidence to these MWNT properties, numerous research groups reported enhanced electrochemical activity on MWNT-enzyme composite modified electrodes as comprehensively reviewed in the literature.<sup>20,21</sup>

To improve the immobilization stability of enzymes on MWNTs, different approaches have been reported in the literature for a multitude of enzymes.<sup>22</sup> Of particular interest to this work are the multicopper oxidases (MCOs) because of their electro-catalytic activity for ORR. Accordingly, many research groups across the

**Received:** October 12, 2011

**Revised:** November 9, 2011

**Published:** November 16, 2011

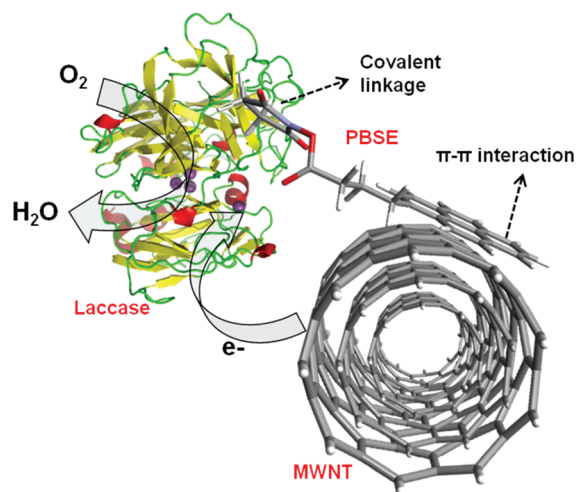


**Figure 1.** Schematic of the bio-nanocomposite where laccase is tethered to MWNT using pyrenebutanoic acid succinimidyl ester (PBSE). Tethering is through a coupled covalent-binding of the protein and a noncovalent sidewall functionalization of MWNT through a  $\pi$ - $\pi$  interaction. The tethered laccase reduces oxygen to water through direct electron transfer.

globe have explored the electro-catalysis of ORR by the MCOs such as ascorbate oxidase, bilirubin oxidase, and laccase.<sup>23–29</sup> Among these MCOs, laccase has received much interest because of its ability to reduce O<sub>2</sub> at high electrochemical potentials and its potential use as cathode catalyst in biological fuel cells.<sup>30,31</sup> Quite a few studies on the electrochemical oxygen reduction by laccase have been reported in the literature.<sup>32–36</sup> However, these studies do not report key kinetic parameters of ORR by laccase, except one where the biomolecular kinetics of mediated enzyme electrode systems were discussed.<sup>36</sup> No such studies have been reported for a direct electrochemical reduction of oxygen by enzyme electrodes.

Our previous work<sup>37</sup> showed high electro-catalytic activity of laccase-MWNT tethered composites for ORR through direct electron transfer. In that work, laccase was molecularly tethered to MWNT using 1-pyrene butanoic acid succinimidyl ester (PBSE) as a tethering agent. As schematically shown in Figure 1, PBSE covalently binds to the laccase on one end and noncovalently to the MWNT on the other end through a  $\pi$ - $\pi$  interaction.<sup>38</sup> The MWNT served as the immobilization support for laccase while providing the added advantage of high electrical conductivity and large surface area for electro-catalysis. In this paper, we present the experimental results from our comprehensive kinetic analysis of the tethered laccase-MWNT composite catalysts using rotating ring-disk electrode (RRDE) studies. A likely reaction mechanism for ORR by laccase in the kinetic region has been postulated and substantiated. The various electro-kinetic and mechanistic parameters for the bio-nanocomposite catalyzed ORR have also been quantified for the first time for direct enzyme electro-catalysis.

## EXPERIMENTAL SECTION

**Materials.** MWNTs, 10 nm diameter and 1.5  $\mu$ m length (Dropsens, Spain) were used as the immobilization support. PBSE (Anaspec Inc., Fremont, CA) was used as the hetero-bifunctional tethering agent. *N,N*-dimethyl formamide (DMF)

(Thermo Fisher, NJ) was the solvent used for MWNTs and PBSE preparation. Laccase from *Trametes versicolor* (Sigma, St. Louis, MO) was the enzyme used for ORR electro-catalysis. Industrial grade O<sub>2</sub> (Airgas, Atlanta, GA) was used for the electrochemical experiments. The electrolyte used was 100 mL of 100 mM potassium phosphate buffer (pH 5.8). This phosphate buffer electrolyte was prepared using monobasic and dibasic potassium phosphates (VWR, Suwanee, GA). Distilled and deionized water (18 M $\Omega$  conductivity) was used to prepare all the solutions.

**Apparatus.** RRDE setup (PINE Instruments Inc., Grove City, PA) was used to carry out the electrochemical ORR kinetic studies. The set up is made of glassy carbon disk and platinum ring electrodes mounted on a rotating shaft controlled by an RPM controller. An electrode polishing kit consisting of a polishing pad and 0.3  $\mu$ m pore size alumina powder (CH Instruments Inc., Austin, TX) was used to polish the ring and disk electrodes. A glass voltammetry cell of 125 mL capacity was used to carry out all the experiments. Ag/AgCl reference and platinum mesh counter electrodes were obtained from CH Instruments Inc., Austin, TX. A potentiostat model CHI-920c (CH Instruments Inc., Austin, TX) was used to control both the disk and ring potentials. All the potentials were reported with respect to the Ag/AgCl reference.

**Laccase-MWNT Composite Preparation.** The glassy carbon disk and the platinum ring were polished with 0.3  $\mu$ m pore size alumina powder and then washed thoroughly with water. The cleaned rotating disk electrode was coated with known quantity of MWNT suspension, and dried at 70 °C. The MWNT coated electrode was then incubated with PBSE solution of a known concentration for 15 min. The excess tethering agent on the electrode was washed away using DMF and then with phosphate buffer (pH 7). After washing, laccase from a solution of known concentration was immobilized on the MWNT-PBSE modified electrode by drop coating and incubating for 30 min.

**Electrochemical Characterization.** All electrochemical measurements were done in a 150 mL voltammetry cell containing potassium phosphate buffer as electrolyte. The electrolyte was initially saturated with O<sub>2</sub> and then the experiments were carried out using laccase-MWNT composite modified RRDE. Linear sweep voltammograms were obtained for the disk and ring at different rotation rates, where the disk potential was swept from 0.8 to 0 V at a scan rate of  $-0.01$  V s<sup>-1</sup>, and the ring potential was kept constant at 1 V. The Tafel region sweep experiment was carried out for the disk electrode in the potential range of  $-0.2$  to  $+0.2$  V versus the onset potential for oxygen reduction. The kinetic parameters such as Tafel slope, number of electrons, and rate constants were calculated using voltammogram results and Tafel plot data.

## RESULTS AND DISCUSSION

**Optimization of Bio-Nanocomposite Preparation.** The preparation condition and composition of laccase-MWNT bio-nanocomposite was optimized through a series of experiments as explained below. The first set of optimization experiments was carried out by varying the MWNT loading in the bio-nanocomposite to study the ORR. The various MWNT loadings tried on the disk electrode surface were 0, 0.25, 0.5, and 0.8 mg cm<sup>-2</sup>, in which 0.8 mg cm<sup>-2</sup> gave the highest reduction current for ORR at high potentials when tested using a cyclic voltammogram (CV). Similar optimization studies were carried out for PBSE

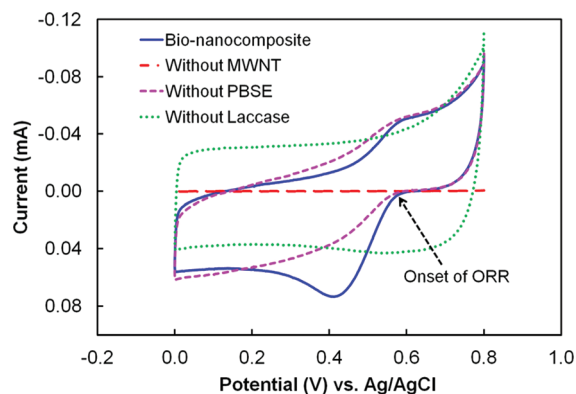


**Figure 2.** Comparison of CVs of the complete and incomplete bio-nanocomposite obtained in  $O_2$ -saturated phosphate buffer (pH 5.8. Scan rate is  $10 \text{ mV s}^{-1}$ ).

(incubating solution concentration =  $1\text{--}10 \text{ mM}$ ) and laccase (incubating solution concentration =  $5\text{--}20 \text{ mg mL}^{-1}$ ). The optimized concentration of PBSE and laccase used for incubation was  $5 \text{ mM}$  and  $10 \text{ mg mL}^{-1}$ , respectively. The optimizations were based on high achievable currents for ORR in the kinetic region of the CVs (see Supporting Information, Figure A1). The open circuit potential (OCP) obtained for the optimized bio-nanocomposite modified electrode was  $0.63 \text{ V}$  vs Ag/AgCl. The slope of the ORR curve was also higher in the optimized condition, which is evident from the lowest difference between the OCP and half peak potentials (see Supporting Information, Figure A1).

For all our electrochemical kinetic studies, we prepared the bio-nanocomposite using the optimized preparation conditions. Figure 2 compares the CVs of the complete optimized bio-nanocomposite (laccase, PBSE, and MWNT) with that of incomplete composites (i.e., without one of the components). As seen from Figure 2, the electro-catalytic activity of the complete bio-nanocomposite was the highest, evidenced from the steep oxygen reduction cathodic wave in the CV with an onset potential of  $0.55 \text{ V}$  and a peak potential of  $0.47 \text{ V}$ . The voltammograms also reveal that the absence of any one of the components dramatically changed the shape of the cathodic reduction wave. For example, in the absence of laccase, there was no indication of any  $O_2$  reduction by the composite as both anodic and cathodic waves showed no faradaic current. In the absence of MWNT, the capacitance was too low (because of low surface area of the composite) to notice any  $O_2$  reduction activity. In the absence of PBSE, the laccase was only physically adsorbed onto MWNT with weak interaction and poor direct electron transfer. As a result, the ORR activity was significantly less compared to that of the complete bio-nanocomposite.

**Hydrodynamic Studies.** RRDE studies were carried out to derive the electro-kinetics of ORR by the laccase-MWNT bio-nanocomposite. A schematic of the RRDE hydrodynamics for ORR is shown in Figure 3a. The convection in the voltammetry cell allows faster transport of the reactant ( $O_2$ ) from the bulk to the disk electrode.<sup>39</sup> At the disk,  $O_2$  is reduced, and the products are immediately transported away toward the ring by convection because of the rotating disk. Because the ring was held at sufficiently high potential ( $1 \text{ V}$  vs Ag/AgCl), any  $H_2O_2$  formed at the disk as a result of incomplete  $O_2$  reduction oxidizes to water at the ring and is represented by ring current. The experimentally measured disk current ( $I_D$ ) and ring current

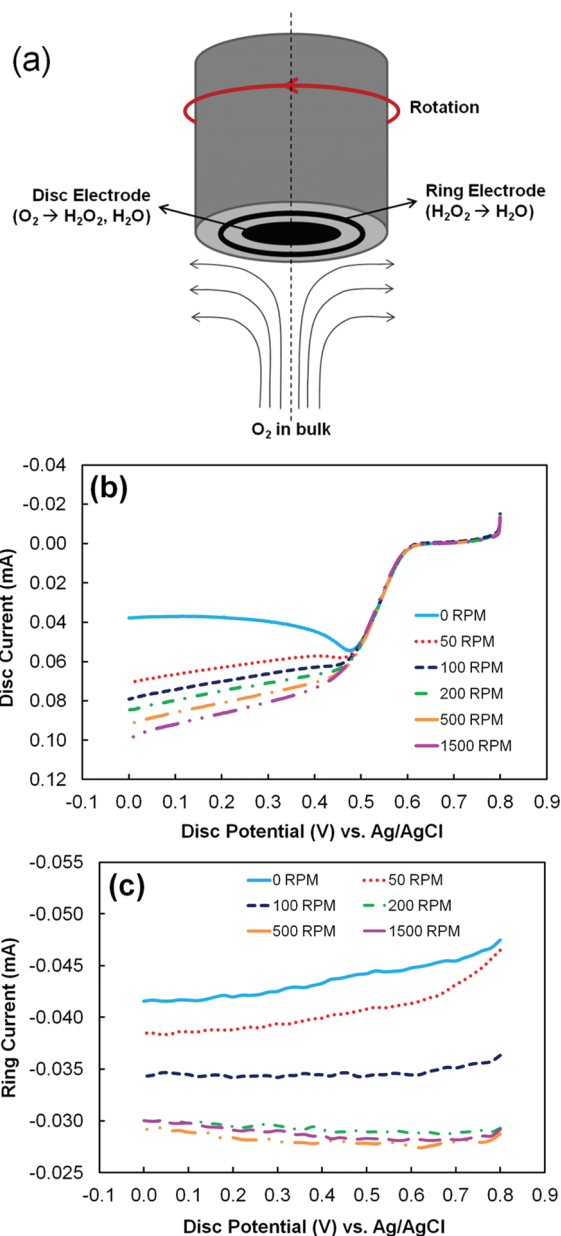


**Figure 3.** Rotating ring disk electrode measurements using linear sweep voltammetry at various disk rotation speeds from  $0.8$  to  $0 \text{ V}$  at the scan rate of  $10 \text{ mV s}^{-1}$ . (a) Hydrodynamics at the rotating-ring disk electrode. (b) Plot of disk current ( $I_D$ ) vs disk potential. (c) Plot of ring current ( $I_R$ ) vs disk potential.

( $I_R$ ) at different disk rotation speeds ( $0\text{--}1500 \text{ RPM}$ ) are given in Figures 3b and 3c, respectively. In the RRDE results, the OCP of ORR measured on the disk at  $0 \text{ RPM}$  was  $0.63 \text{ V}$  indicating a high redox activity by the catalyst. With no rotation, the cathodic wave of CV showed  $O_2$  reduction at and below  $0.55 \text{ V}$  with a steep slope peaking at  $0.47 \text{ V}$ . Below this voltage, the disk current started to decrease indicating the mass transport limitation for  $O_2$  in the solution. At higher disk rotation speeds, the mass transfer limitation for  $O_2$  transport to disk surface was minimized resulting in high limiting currents. While the increasing RPMs increased the limiting current ( $I_L$ ) of ORR, the slope of the cathodic reduction wave remained constant ( $37 \mu\text{A V}^{-1}$ ) indicating stable catalytic activity at all the rotation

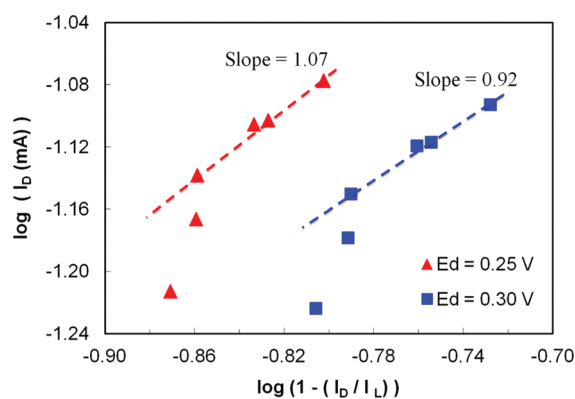


**Figure 4.** Determination of the overall order of the reaction with respect to oxygen for ORR by laccase-MWNT bio-nanocomposite.

speeds. The comparison of the  $I_D$  for the highly active bio-nanocomposite catalyst with a less active enzyme catalyst at a rotation speed of 100 RPM is shown in Supporting Information, Figure A2. The less active catalyst composite was prepared using a partially denatured laccase. The figure shows a clear difference in the cathodic wave slopes indicating that the laccase retained its electro-catalytic activity inside the bio-nanocomposite. The steepness of the ORR curve obtained for the bio-nanocomposite consisting of laccase-MWNT provided clear evidence that the tethered conjugates possess excellent direct electron transfer capabilities as qualitatively determined in our previous work.<sup>37</sup>

**Order of the Reaction.** The order of the ORR at the bio-nanocomposite modified disk electrode was determined by eq 1.

$$\log I_D = \log I_{kin} + p \log \left( 1 - \frac{I_D}{I_L} \right) \quad (1)$$

where  $I_D$  is the disk current,  $p$  is the order of the reaction,  $I_{kin}$  is kinetic current of the disk electrode given by  $I_{kin} = (I_L \times I_D) / (I_L - I_D)$ .<sup>5</sup> The equation shows the relationship between  $I_D$  and  $I_L$  for different RPM, where  $I_L$  is the limiting current at which the rate of  $O_2$  reduction equals the rate of  $O_2$  diffusion.  $I_{kin}$  is the intercept of the graph given in Figure 4. The values of  $I_D$  and  $I_L$  were obtained from the voltammograms of rotation speeds ranging from 50 to 1500 RPM at 0.25 and 0.3 V. High rotation speeds were chosen for calculating  $p$  because they have low  $O_2$  diffusion control effects, which increases the precision of  $I_L$  calculation.<sup>40</sup> Similarly the potential range 0.25 to 0.3 V was chosen for calculations to ensure that the values are outside the kinetic limited region. The plots of  $\log I_D$  versus  $\log(1 - I_D/I_L)$  in Figure 4 were linear with the slope values nearly unity, showing that ORR at the laccase-MWNT modified electrode obeys first order kinetics. The kinetic analysis such as the Levich analysis, the Koutecky–Levich analysis, and rate constants are given in the following sections based on first order kinetics of ORR.

**Effect of Rotation Speed.** The voltammograms given in the previous sections were used to understand the relationship between  $I_L$  and concentration of  $O_2$  as a function hydrodynamics (i.e., RPM). This relationship can be explained by the Levich eq 2.

$$I_L = 0.62nFAD^{2/3}v^{-1/6}\omega^{1/2}c \quad (2)$$

where  $I_L$  is the limiting current,  $n$  is the number of electrons transferred per molecule of analyte,  $F$  is faraday's constant,  $A$  is

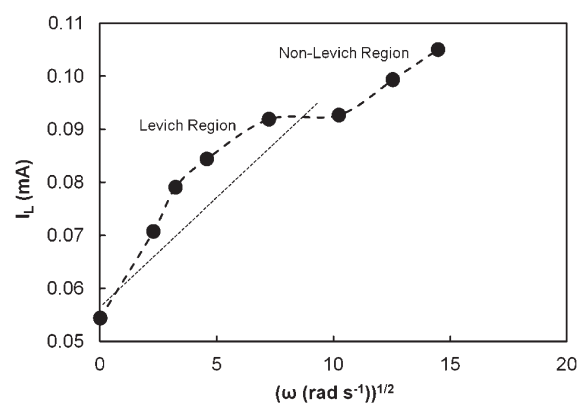


**Figure 5.** Plot showing the Levich and Non-Levich regions for ORR by bio-nanocomposite modified disk electrode. Rotation speeds ranged from 0 to 2000 RPM. The linear part represents the Levich region, and the nonlinear part is the non-Levich region.

the electrode surface area ( $0.196 \text{ cm}^2$ ),  $D$  is the diffusion coefficient of  $O_2$  ( $2.6 \times 10^{-5} \text{ cm}^2 \text{ s}^{-1}$ ),<sup>41</sup>  $v$  is the kinematic viscosity,  $\omega$  is the frequency of rotation speed, and  $c$  is the analyte concentration ( $1.22 \text{ mM}$ ).<sup>42</sup> The  $I_L$  values were obtained from the voltammograms of the disk electrode. Because of the difficulty in interpreting the precise value of the limiting current from experimental data, the  $I_L$  for 0 RPM was measured at a potential of 0.48 V (where the disk current peaks), and for all other rotation speeds it was measured at 0 V. The Levich and non-Levich regions of the laccase-MWNT composite catalyzed ORR is given by the plot between  $I_L$  and  $\omega^{1/2}$  as shown in Figure 5. The linear region in the plot represents the Levich region where the flow was laminar and Levich kinetics applies. Converting the  $\omega^{1/2}$  of linear region to rotation speed gives 0 to 500 RPM as the Levich region. The nonlinear region is the non-Levich region where the free diffusion of  $O_2$  to the electrode surface was hindered by heavy turbulence. The limiting current in the non-Levich region is not a strong function of  $O_2$  concentration. On the basis of these above results, all other following kinetic studies were carried out within Levich region.

**Number of Electrons.** The number of electrons involved in the ORR laccase-MWNT modified disk electrode was calculated by the Koutecky–Levich eq 3 for a first order reaction<sup>5</sup>

$$\frac{1}{I_D} = \frac{1}{I_{kin}} + \frac{1}{B\omega^{1/2}} \quad (3)$$

where  $I_D$  is the disk current,  $I_{kin}$  is the kinetic current,  $\omega$  is the rotation speed, and  $B$  is the Levich slope given by eq 4.

$$B = 0.62nFACD^{2/3}v^{-1/6} \quad (4)$$

where  $n$  is the number of electrons transferred,  $F$  is the Faraday's constant,  $A$  is the electrode surface area,  $c$  is the bulk concentration of  $O_2$  in the electrolyte,  $D$  is the diffusion coefficient of  $O_2$ , and  $v$  is the kinematic viscosity of the electrolyte ( $9.13 \times 10^{-3} \text{ cm}^2 \text{ s}^{-1}$ ).<sup>11</sup> To calculate the  $n$  value, Koutecky–Levich plots ( $1/\omega^{1/2}$  vs  $1/I_D$ ) for different RPM in the kinetic region were plotted as shown in Figure 6a. The Koutecky–Levich plots for various potentials (0.4, 0.35, 0.3, and 0.25 V) yielded straight lines with slopes of 11.1, 11.9, 11.9, and 11.8  $\text{mA s}^{-1/2}$  respectively. By substituting these slope values in eq 4, the number of

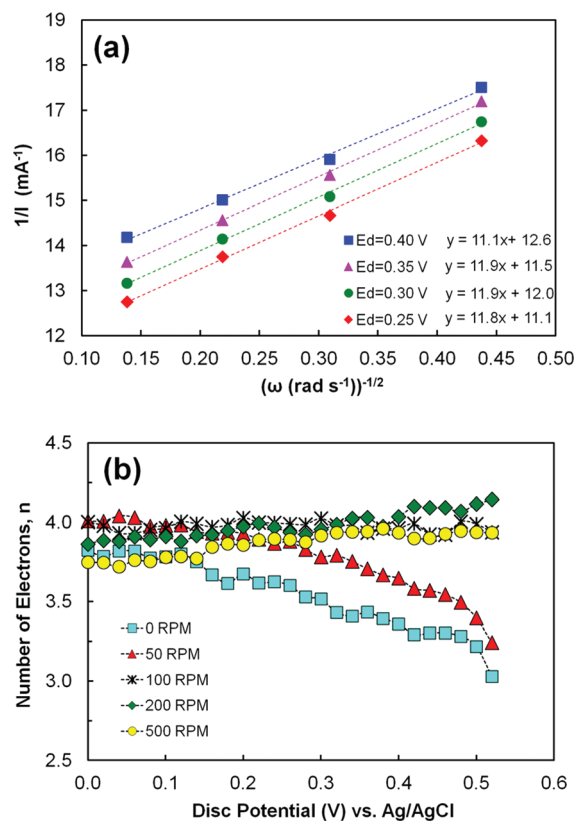


**Figure 6.** (a) Koutecky–Levich plots at various disk potentials (0.25–0.4 V) outside the kinetics limited region. (b) Number of electrons as a function of disk potential in the O<sub>2</sub> reduction region (0–0.525 V).

electrons transferred during ORR at bio-nanocomposite was calculated to be between 3.8 and 4.0. These calculated values for  $n$  were validated using  $I_R$  data in the following section.

**Ring Current Analysis.** The variation of  $I_R$  with disk potential at different RPM as shown in Figure 3b indicates a difference in H<sub>2</sub>O<sub>2</sub> oxidation at the ring electrode. The  $I_R$  was lower in the diffusion limiting region when compared to the region above the OCP. This is due to the activation polarization at high potentials where the laccase could not “kick-start” the direct four-electron reduction of O<sub>2</sub> resulting in more H<sub>2</sub>O<sub>2</sub> formation. The ring currents showed also a decrease in magnitude with increase in RPM, but at very high RPM the  $I_R$  was constant. Besides the high electro-catalytic activity exhibited by the laccase-MWNT composite catalyst, the ring and disk currents were comparable in magnitude. This could be because of a simultaneous O<sub>2</sub> and H<sub>2</sub>O<sub>2</sub> oxidation at the platinum ring, which was held at sufficiently high overpotential for both these reactions to happen at the operating pH. A detailed analysis of the ring current data has been done to understand the extent of H<sub>2</sub>O<sub>2</sub> formation at the disk because of incomplete O<sub>2</sub> reduction. The total number of electrons exchanged per molecule of O<sub>2</sub> directly relates to the extent of the preferred four electron ORR. The number of electrons was calculated from the ring and disk currents using eq 5

$$n = \frac{4}{1 + \frac{I_R}{NI_D}} \quad (5)$$

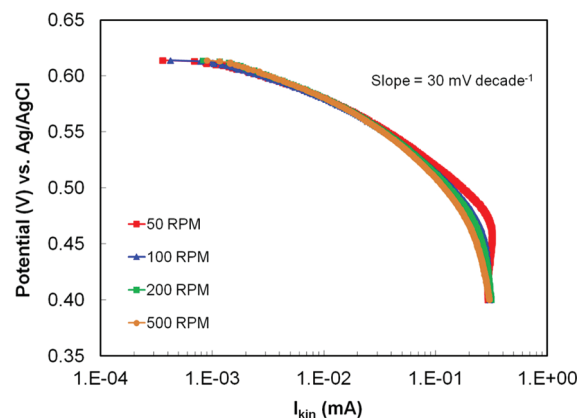


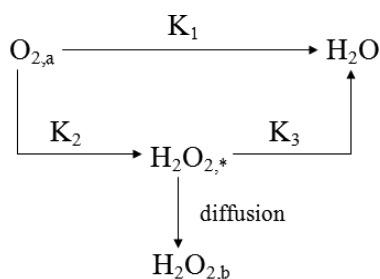
**Figure 7.** Tafel plot obtained from the calculated kinetic current values at different RPM in the kinetic region.

where  $N$  is the collection efficiency. It refers to the fraction of the H<sub>2</sub>O<sub>2</sub> formed at the disk that was collected at the ring. It is purely a geometric parameter that was experimentally determined to be 0.256 by the manufacturer for our RRDE setup.<sup>6</sup> The potential range used to calculate the number of electrons involved in O<sub>2</sub> reduction was 0–0.525 V, which was the O<sub>2</sub> reduction region. The calculated values of  $n$  for different RPM were plotted against  $I_D$  as given in Figure 6b. The plot shows that the number of electrons involved in ORR varied between 3.8 and 4 at high rotation speeds indicative of a direct four-electron reduction with minimum intermediate formation (H<sub>2</sub>O<sub>2</sub>). The result supports the argument that laccase-MWNT composites possess excellent electro-catalytic activity for O<sub>2</sub> reduction.

**Electro-Catalytic Activity.** The electro-catalytic activity of the bio-nanocomposite toward ORR can also be evaluated using Tafel slopes obtained in the kinetic region of O<sub>2</sub> reduction from the linear sweep voltammograms. Generally, the Tafel slope is the slope of the linear region in an  $I_D$  versus  $I_{kin}$  plot. The theoretical value of the Tafel slope for a four-electron reduction is 15 mV (= 59 mV/ $n$ ) per decade change of  $I_{kin}$ . The closer the experimental value is to this number, the better is the electro-catalyst for ORR.<sup>42</sup> Figure 7 shows the Tafel plot for kinetic region of ORR at the bio-nanocomposite, where the linear region is from  $1 \times 10^{-3}$  to  $1 \times 10^{-2}$  mA. The obtained Tafel slope from the above-mentioned region was 31 mV per decade change of  $I_{kin}$ , and was constant for all RPM inside the Levich region. This obtained Tafel slope for ORR on the disk electrode was lower than the value obtained in our previous work.<sup>37</sup> The difference between the values could be due to the difference in the type of the electrode used for bio-nanocomposite modification: glassy carbon in this work whereas porous carbon paper in the previous work.<sup>37</sup> However, the Tafel slope for the laccase-MWNT composite is significantly lower than the values for metallic ORR catalysts reported in the literature that range from 60 to 140 mV per decade,<sup>5,43</sup> another metric supporting the evidence of high electro-activity by the bio-nanocomposite. For comparison, the electro-catalytic activity of a less active laccase containing bio-nanocomposite for ORR (see Supporting Information, Figure A2) was studied in a parallel experiment. The result for the less active composite gave a Tafel slope >500 mV dec<sup>-1</sup> of  $I_{kin}$  which is dramatically different from that of the active composite.

**Electrochemical Rate Constants.** The proposed reaction pathway of ORR in the bio-nanocomposite modified electrode

is given by the eq 6, where  $K_1$ ,  $K_2$ , and  $K_3$  are the reaction rate constants for each of the reactions shown in the equation.



The  $O_{2,a}$  in the above equation is the oxygen available to the enzyme catalyst for reduction at the disk.  $H_2O_{2,*}$  is the hydrogen peroxide formed as an intermediate at the disk because of incomplete  $O_2$  reduction. A portion of the adsorbed  $H_2O_{2,*}$  on the disk further gets converted into water, and the remaining diffuses into the bulk electrolyte solution as  $H_2O_{2,b}$ . This reaction model described in eq 6 is similar to the one reported by Damjanovic et al.<sup>44</sup> According to this model, the rate constants of the ORR pathways were calculated by the following equations.

$$K_1 = S_2 Z_1 \frac{I_1 N - 1}{I_1 N + 1} \quad (7)$$

$$K_2 = \frac{2Z_1 S_2}{I_1 N + 1} \quad (8)$$

$$K_3 = \frac{Z_2 N S_1}{I_1 N + 1} \quad (9)$$

$$Z_1 = 0.62 D_1^{2/3} \nu^{-1/6} \quad (10)$$

$$Z_2 = 0.62 D_2^{2/3} \nu^{-1/6} \quad (11)$$

where  $S_1$  and  $I_1$  are the slope and the intercept of the plot of  $I_D/I_R$  versus  $\omega^{-1/2}$ ,  $S_2$  is the slope of  $I_{DL}/(I_{DL} - I_D)$  versus  $\omega^{-1/2}$ . These plots are shown in the Supporting Information, Figure A3. The  $I_D/I_R$  versus  $\omega^{-1/2}$  was plotted at 0.25 V, in which the slope  $S_1$  is 4.50 and the intercept is  $-3.77$ . Similarly, the slope of  $I_{DL}/(I_{DL} - I_D)$  versus  $\omega^{-1/2}$  is 2.24. Applying these values in the above equations gives the values of  $K_1$ ,  $K_2$ , and  $K_3$  as  $1.46 \times 10^{-3} \text{ m s}^{-1}$ ,  $1.49 \times 10^{-3} \text{ m s}^{-1}$ , and  $2.27 \times 10^{-4} \text{ m s}^{-1}$ , respectively. The values of  $K_1$  and  $K_2$  were similar in magnitude indicating that the rate constants for both water and peroxide formation reactions were similar. The rate constant for  $O_2$  reduction by laccase-MWNT composite catalysts were an order of magnitude higher than for oxygen reduction on metallic surfaces,<sup>45</sup> indicating that enzymes have higher electro-catalytic activity than metallic catalysts on a per catalytic site basis as suggested by Barton et al.<sup>25</sup> For comparison the same reaction model (eq 6) calculations were applied for less active laccase containing bio-nanocomposite. For less active laccase (Supporting Information, Figure A2), the obtained values were  $1.03 \times 10^{-4} \text{ m s}^{-1}$ ,  $1.1 \times 10^{-4} \text{ m s}^{-1}$ , and  $4.2 \times 10^{-6} \text{ m s}^{-1}$  for  $K_1$ ,  $K_2$ , and  $K_3$  respectively, approximately 15 times lower than that for the active laccase-MWNT composites.

**Electron Transfer Rate.** Electron transfer between an electrode and the analyte happens at a finite rate depending on the

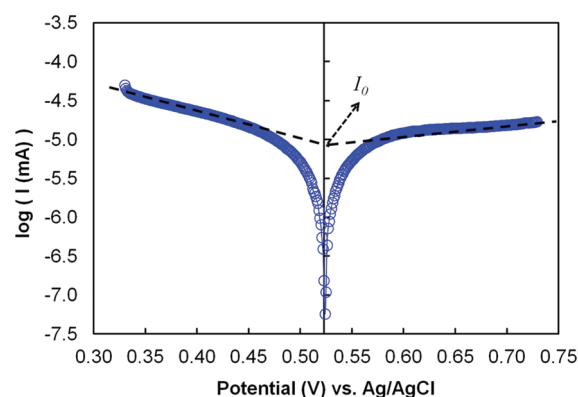


**Figure 8.** Linear sweep voltammograms showing Tafel regions at no rotation for the laccase-MWNT in phosphate buffer (pH 5.8). The applied potential range was from 0.33 to 0.73 V.

conductivity of the electrode, distance between the electrode and the enzyme redox center, and the electro-activity of the catalyst. The electron transfer rate constant of the ORR on laccase-MWNT modified electrode was calculated by the eq 12.

$$I_0 = nFAK_{et}c \quad (12)$$

where  $I_0$  is the exchange current obtained from Tafel plot,  $n$  is the number of electrons,  $F$  is the Faraday's constant,  $A$  is the electrode surface area,  $K_{et}$  is the electron transfer rate constant,  $c$  is the concentration of the analyte in the bulk solution. Figure 8 represents the plot of  $\log I$  versus overpotential for the electrochemical redox reactions, which can be expressed by eq 13.

$$I = a + b \exp(\eta) \quad (13)$$

where  $a$  and  $b$  are empirical fitting constants and  $\eta$  is the overpotential. For this, the disk electrode was swept between 0.33 to 0.73 V ( $-0.2$  to  $+0.2$  V vs onset potential for ORR) at 0 RPM. Ideally this plot should be linear. However, it appears nonlinear because of the large voltage window used for sweeping the voltage. From the plot in Figure 8,  $I_0$  was calculated by intersecting the tangents at nonlinear regions of the Tafel curve. The obtained values of equilibrium exchange current density ( $I_0$ ) and the electron transfer rate ( $K_{et}$ ) were  $3.3 \times 10^{-5} \text{ A cm}^{-2}$  and  $6.72 \times 10^{-5} \text{ cm s}^{-1}$  respectively.

## CONCLUSION

This paper comprehensively presents the first detailed electrochemical and kinetic studies of ORR by a laccase based composite catalyst. The electro-kinetic parameters for enzyme electro-catalysis through direct electron transfer have been reported for the first time. It was made possible by the successful integration of the enzyme into a bio-nanocomposite catalyst that can be deposited onto disk electrode and retains stability at high rotation speeds. The effect of rotation speed on the  $O_2$  reduction ability revealed that the increase in rotation speed increases the limiting current of  $O_2$ . This indicates that rotation helps overcome the mass transfer limitation occurring at stationary electrodes. The electro-kinetic parameters such as order of reaction, number of electrons transferred per  $O_2$ , Tafel slopes, kinetic rate constant of reactions at the disk electrode, and the electron transfer rate constant have been reported. These electro-kinetic results demonstrated that laccase present in the bio-nanocomposite has high electro-catalytic activity toward ORR. The rate

constant of electrochemical reduction of O<sub>2</sub> by enzyme has been reported for the first time, and it was an order of magnitude higher than that reported for other metal catalysts, indicating excellent electro-catalytic activity of the enzyme composite catalysts. The properties reported in this work can be used as a benchmark for developing laccase based catalysts for biofuel cell and electrochemical sensor applications.

## ■ ASSOCIATED CONTENT

**S Supporting Information.** Further details are given in Figures A1–A3. This material is available free of charge via the Internet at <http://pubs.acs.org>.

## ■ AUTHOR INFORMATION

### Corresponding Author

\*E-mail: [rama@uga.edu](mailto:rama@uga.edu). Fax: +1-706-542-3804.

### Funding Sources

The authors would like to acknowledge the University of Georgia for its financial support.

## ■ REFERENCES

- (1) Damjanovic, A.; Brusica, V. *Electrochim. Acta* **1967**, *12*, 615.
- (2) Damjanovic, A.; Genshaw, M. A.; Bockris, J. O. M. *J. Electrochem. Soc.* **1967**, *114*, 466.
- (3) Damjanovic, A.; Sepa, D. B.; Vojnovic, M. V. *Electrochim. Acta* **1979**, *24*, 887.
- (4) Sepa, D. B.; Vojnovic, M. V.; Damjanovic, A. *Electrochim. Acta* **1980**, *25*, 1491.
- (5) Gojkovic, S. L.; Gupta, S.; Savinell, R. F. *J. Electroanal. Chem.* **1999**, *462*, 63.
- (6) Gojkovic, S. L.; Gupta, S.; Savinell, R. F. *Electrochim. Acta* **1999**, *45*, 889.
- (7) Hsueh, K. L.; Chin, D. T.; Srinivasan, S. *J. Electroanal. Chem.* **1983**, *153*, 79.
- (8) Mukerjee, S.; Srinivasan, S. *J. Electroanal. Chem.* **1993**, *357*, 201.
- (9) Anastasijević, N. A.; Vesović, V.; Adžić, R. R. *J. Electroanal. Chem.* **1987**, *229*, 305.
- (10) Anastasijević, N. A.; Vesović, V.; Adžić, R. R. *J. Electroanal. Chem.* **1987**, *229*, 317.
- (11) Anastasijević, N. A.; Dimitrijević, Z. M.; Adžić, R. R. *Electrochim. Acta* **1986**, *31*, 1125.
- (12) Gewirth, A. A.; Thorum, M. S. *Inorg. Chem.* **2010**, *49*, 3557.
- (13) Barton, S. C.; Gallaway, J.; Atanassov, P. *Chem. Rev.* **2004**, *104*, 4867.
- (14) Armstrong, F. A.; Hill, H. A. O.; Walton, N. J. *Q. Rev. Biophys.* **1985**, *18*, 261.
- (15) Joshi, P. P.; Merchant, S. A.; Wang, Y.; Schmidtke, D. W. *Anal. Chem.* **2005**, *77*, 3183.
- (16) Ellerby, L.; Nishida, C.; Nishida, F.; Yamanaka, S.; Dunn, B.; Valentine, J.; Zink, J. *Science* **1992**, *255*, 1113.
- (17) Cosnier, S. *Biosens. Bioelectron.* **1999**, *14*, 443.
- (18) Ivnitski, D.; Artyushkova, K.; Rincón, R. A.; Atanassov, P.; Luckarift, H. R.; Johnson, G. R. *Small* **2008**, *4*, 357.
- (19) Mazur, M.; Krywko-Cendrowska, A.; Krysinski, P.; Rogalski, J. *Synth. Met.* **2009**, *159*, 1731.
- (20) Merkoçi, A.; Pumera, M.; Llopis, X.; Pérez, B.; del Valle, M.; Alegret, S. *TrAC, Trends Anal. Chem.* **2005**, *24*, 826.
- (21) Wang, J. *Electroanalysis* **2005**, *17*, 7.
- (22) Feng, W.; Ji, P. *Biotechnol. Adv.* **2011**, *29*, 889.
- (23) Bilewicz, R.; Opallo, M. In *Fuel Cell Science: Theory, Fundamentals, and Biocatalysis*; Więckowski, A., Nørskov, J., Eds.; John Wiley & Sons: New York, 2010; Vol. 4, p 169.
- (24) Blanford, C.; Foster, C.; Heath, R.; Armstrong, F. *Faraday Discuss.* **2009**, *140*, 319.
- (25) Barton, S. C.; Kim, H.-H.; Binyamin, G.; Zhang, Y.; Heller, A. *J. Am. Chem. Soc.* **2001**, *123*, 5802.
- (26) Shleev, S.; Tkac, J.; Christenson, A.; Ruzgas, T.; Yaropolov, A. I.; Whittaker, J. W.; Gorton, L. *Biosens. Bioelectron.* **2005**, *20*, 2517.
- (27) Atanassov, P.; Apblett, C.; Banta, S.; Brozik, S.; Barton, S. C.; Cooney, M.; Liaw, B. Y.; Mukerjee, S.; Minteer, S. D. *Electrochem. Soc. Interface* **2007**, *16*, 28.
- (28) Scheller, F. W.; Wollenberger, U.; Lei, C.; Jin, W.; Ge, B.; Lehmann, C.; Lisdat, F.; Fridman, V. *Rev. Mol. Biotechnol.* **2002**, *82*, 411.
- (29) Solomon, E. I.; Augustine, A. J.; Yoon, J. *Dalton Trans.* **2008**, 3921.
- (30) Palmore, G. T. R.; Kim, H.-H. *J. Electroanal. Chem.* **1999**, *464*, 110.
- (31) Farneth, W. E.; D'Amore, M. B. *J. Electroanal. Chem.* **2005**, *581*, 197.
- (32) Tarasevich, M. R.; Yaropolov, A. I.; Bogdanovskaya, V. A.; Varfolomeev, S. D. *J. Electroanal. Chem. Interfacial Electrochem.* **1979**, *104*, 393.
- (33) Thorum, M. S.; Anderson, C. A.; Hatch, J. J.; Campbell, A. S.; Marshall, N. M.; Zimmerman, S. C.; Lu, Y.; Gewirth, A. A. *J. Phys. Chem. Lett.* **2010**, *1*, 2251.
- (34) Frascioni, M.; Favero, G.; Boer, H.; Koivula, A.; Mazzei, F. *Biochim. Biophys. Acta* **2010**, *1804*, 899.
- (35) Yaropolov, A.; Shleev, S.; Zaitseva, E.; Emnéus, J.; Marko-Varga, G.; Gorton, L. *Bioelectrochem.* **2007**, *70*, 199.
- (36) Gallaway, J. W.; Calabrese Barton, S. A. *J. Am. Chem. Soc.* **2008**, *130*, 8527.
- (37) Ramasamy, R. P.; Luckarift, H. R.; Ivnitski, D. M.; Atanassov, P. B.; Johnson, G. R. *Chem. Commun.* **2010**, *46*, 6045.
- (38) Chen, R. J.; Zhang, Y.; Wang, D.; Dai, H. *J. Am. Chem. Soc.* **2001**, *123*, 3838.
- (39) Levich, V. G. *Physicochemical Hydrodynamics*; Prentice-Hall Inc.: Englewood Cliffs, NJ, 1962.
- (40) Monk, P. M. S. *Fundamentals of Electroanalytical Chemistry*; John Wiley & Sons Ltd.: New York, 2001.
- (41) Millington, R. J. *Science* **1955**, *122*, 1090.
- (42) Gnanamuthu, D. S.; Petrocelli, J. V. *J. Electrochem. Soc.* **1967**, *114*, 1036.
- (43) Jiang, T.; Brisard, G. M. *Electrochim. Acta* **2007**, *52*, 4487.
- (44) Damjanovic, A.; Dey, A.; Bockris, J. O. M. *Electrochim. Acta* **1966**, *11*, 791.
- (45) Jakobs, R. C. M.; Janssen, L. J. J.; Barendrecht, E. *Electrochim. Acta* **1985**, *30*, 1085.